

TOWARDS IMAGE-BASED HOMOGENIZATION BY COMBINING SCANNING TECHNIQUES AND REDUCED ORDER MODELING

E. Lopez*, E. Abisset-Chavanne, C. Ghnatios, S. Comas-Cardona, C. Binetruy, F. Chinesta

GeM Institute, UMR CNRS, Ecole Centrale de Nantes, 1 rue de la Noe, BP 92101, F-44321 Nantes cedex 3, France

** Corresponding Author: elena.lopez-tomas@ec-nantes.fr*

Keywords: Image-based simulation, Homogenization, Reduced order model, Predictor-Corrector method

Abstract

In the numerical modeling of composite materials and structures, microscopic heterogeneities introduce the need for defining homogenized properties depending on microscopic details. Real time image-based calculations in the framework of the on-line control of manufacturing processes demands the prediction of the local homogenized properties of a heterogeneous material at different scanning scales, as fast as possible for a given acceptable error. Therefore, model reduction techniques open new routes for performing such kinds of efficient high-resolution homogenization.

In this work we propose different reduced order models of thermal conductivities of heterogeneous microstructures, with low and high contrast between both materials, and then we extend the methodology for addressing the homogenization of mechanical properties or the one related to the flow in porous media.

1. Introduction

Numerical homogenization problems can be solved with geometrical data coming from high-resolution images. However, digital images may contain a huge amount of information that is difficult to handle efficiently in numerical models. So image-based computation requires advanced numerical techniques to be developed. Alternatively it raises the question of the minimum resolution of images to predict an effective property with a sufficient accuracy which in turn raises the question of the acceptable error. It is still an open question in composite materials for properties of interest such as thermal conductivity, elasticity or permeability for instance.

In this work we propose a first approach using model reduction techniques to provide compact representations of these images and facilitate efficient computations of the microstructure-property relations.

2. Thermal homogenization

Let \mathcal{M} be a microstructure occupying the volume w at position $\mathbf{X} \in \Omega$. Points in $w(\mathbf{X})$ will be denoted by \mathbf{x} . We do not consider here the problem related to the definition of the representative volume element [4]. If we consider a thermal problem, the microstructure is defined by the thermal conductivity tensor $\mathbf{k}(\mathbf{x})$. We are in the case of a material composed of two phases, so we will have two different values for the components of $\mathbf{k}(\mathbf{x})$ (depending on the position \mathbf{x}), each phase is assumed homogeneous and isotropic.

From now we assumed that the conductivity field is known everywhere in w , that is $\mathbf{k}(\mathbf{x} \in w)$ is known. The crucial question being to predict the homogenized conductivity $\mathbf{K}(\mathbf{X})$. Note than even if each phase is assumed homogeneous and isotropic, the homogenized material could be heterogeneous and anisotropic, depending on the relative distribution of both phases.

In the following we propose a homogenization technique for relating the macroscopic thermal flux $\mathbf{Q}(\mathbf{X})$ and temperature gradient $\mathbf{G}(\mathbf{X})$ at \mathbf{X} according to:

$$\mathbf{Q}(\mathbf{X}) = -\mathbf{K}(\mathbf{X}) \cdot \mathbf{G}(\mathbf{X}) \quad (1)$$

where $\mathbf{K}(\mathbf{X})$ is the searched homogenized thermal conductivity.

At the microscopic level the relation between the local gradient $\mathbf{g}(\mathbf{x})$ and the local heat flux $\mathbf{q}(\mathbf{x})$ is perfectly defined from the local conductivity tensor $\mathbf{k}(\mathbf{x})$ and reads:

$$\mathbf{q}(\mathbf{x}) = -\mathbf{k}(\mathbf{x}) \cdot \mathbf{g}(\mathbf{x}) \quad (2)$$

We assume a localization tensor $\mathbf{L}(\mathbf{x}, \mathbf{X})$ relating the local $\mathbf{g}(\mathbf{x})$ and the macroscopic $\mathbf{G}(\mathbf{X})$ temperature gradients known for a while. Several approaches are proposed in the literature to define this tensor, according to the choice of the boundary conditions. Our objective here is not to discuss this choice, for this purpose the interested reader can find some details in [3]. We have selected the approach in which the localization tensor is defined from:

$$\mathbf{g}(\mathbf{x}) = \mathbf{L}(\mathbf{x}, \mathbf{X}) \cdot \mathbf{G}(\mathbf{X}) \quad (3)$$

Averaging Eq. (2):

$$\begin{aligned} \mathbf{Q}(\mathbf{X}) = \langle \mathbf{q}(\mathbf{x}) \rangle &= \frac{1}{|w|} \int_w \mathbf{q}(\mathbf{x}) \, d\mathbf{x} = -\langle \mathbf{k}(\mathbf{x}) \cdot \mathbf{g}(\mathbf{x}) \rangle = \langle \mathbf{k}(\mathbf{x}) \cdot \mathbf{L}(\mathbf{x}, \mathbf{X}) \cdot \mathbf{G}(\mathbf{X}) \rangle = \\ &= \langle \mathbf{k}(\mathbf{x}) \cdot \mathbf{L}(\mathbf{x}, \mathbf{X}) \rangle \cdot \mathbf{G}(\mathbf{X}) \end{aligned} \quad (4)$$

from which we can identify the expression of the homogenized thermal conductivity:

$$\mathbf{K}(\mathbf{X}) = \langle \mathbf{k}(\mathbf{x}) \cdot \mathbf{L}(\mathbf{x}, \mathbf{X}) \rangle \quad (5)$$

Thus, in order to compute the homogenized thermal conductivity tensor we only need to determine before the localization tensor $\mathbf{L}(\mathbf{x}, \mathbf{X})$.

To do so, in $w(\mathbf{X})$ the heat equation results:

$$\nabla \cdot (\mathbf{k}(\mathbf{x}) \cdot \nabla T(\mathbf{x})) = 0 \quad (6)$$

If we have a temperature field $T_1(\mathbf{x})$ such that the gradient of the solution $\mathbf{g}_1(\mathbf{x}) = \nabla T_1$ verifies:

$$\langle \mathbf{g}_1(\mathbf{x}) \rangle = \mathbf{G}_1(\mathbf{X}) = (1, 0)^T \quad (7)$$

and a second one $T_2(\mathbf{x})$ such that:

$$\langle \mathbf{g}_2(\mathbf{x}) \rangle = \langle \nabla T_2(\mathbf{x}) \rangle = \mathbf{G}_2(\mathbf{X}) = (0, 1)^T \quad (8)$$

From the localization tensor definition:

$$\mathbf{g}(\mathbf{x}) = \mathbf{L}(\mathbf{x}, \mathbf{X}) \cdot \mathbf{G}(\mathbf{X}) \quad (9)$$

the first column of $\mathbf{L}(\mathbf{x}, \mathbf{X})$ is $\mathbf{g}_1(\mathbf{x})$ and the second one is $\mathbf{g}_2(\mathbf{x})$.

Thus, we have to define two steady state thermal problems that allow to obtain the two previous particular thermal fields $T_1(\mathbf{x})$ and $T_2(\mathbf{x})$ which define the localization tensor at each position $\mathbf{x} \in w(\mathbf{X})$ in each microstructure.

It is easy to prove that the thermal problems are the following ones:

$$\begin{cases} \nabla \cdot (\mathbf{k}(\mathbf{x}) \cdot \nabla T_1(\mathbf{x})) = 0 \\ T_1(\mathbf{x} \in \partial w) = x \end{cases} \quad (10)$$

which:

$$\langle \mathbf{g}_1(\mathbf{x}) \rangle = \langle \nabla T_1(\mathbf{x}) \rangle = \mathbf{G}_1(\mathbf{X}) = (1, 0)^T \quad (11)$$

and:

$$\begin{cases} \nabla \cdot (\mathbf{k}(\mathbf{x}) \cdot \nabla T_2(\mathbf{x})) = 0 \\ T_2(\mathbf{x} \in \partial w) = y \end{cases} \quad (12)$$

which solution:

$$\langle \mathbf{g}_2(\mathbf{x}) \rangle = \langle \nabla T_2(\mathbf{x}) \rangle = \mathbf{G}_2(\mathbf{X}) = (0, 1)^T \quad (13)$$

To calculate $\mathbf{K}(\mathbf{X})$ we then need to solve two thermal problems using the Finite Element Method. As this is expensive from the computation point of view, we need to reduce our model.

3. Reduced order modeling

Consider a mesh consisting of n nodes, and associate to each node an approximation function (e.g. a shape function in the framework of the finite element method). We thus implicitly define an approximation space wherein a discrete solution of the problem is sought.

In many cases, however, the problem solution lives in a subspace of dimension much smaller than n , and it makes sense to look for a reduced-order model whose solution is computationally

much cheaper to obtain. This constitutes the main idea behind the Proper Orthogonal Decomposition (POD) [1] [2], briefly revisited hereafter.

We are going to construct a reduced basis from a set of \mathcal{N} microstructures (in the numerical experiments that follow we considered $\mathcal{N}= 100$) for computing the homogenized thermal conductivity tensor $\mathbf{K}(\mathbf{X})$ in "real time" for any new microstructure. These \mathcal{N} microstructures can be viewed as the sampling of a composite stuctures or some realisations in a stochastic process.

3.1. Extracting relevant information: the Proper Orthogonal Decomposition

We assume that a numerical approximation of the unknown temperature fields of interest $T_r(\mathbf{x}, t)$, $r = 1, 2$ for the two problems here considered is known at the nodes \mathbf{x}_i of a spatial mesh, with $i \in [1, \dots, n]$. We define T_r as the vector of nodal values for both thermal problems. The main objective of the POD is to obtain the most typical or characteristic structure $\phi_r(\mathbf{x})$ among these $T_r(\mathbf{x})$. For this purpose, we define a set of \mathcal{N} microstructures (in the numerical experiments that follow we considered $\mathcal{N}= 100$) and we consider and solve using the Finite Element Method, for each microstructure the previous two thermal problems, and then we maximize the scalar quantities:

$$\alpha_r = \frac{\left[\sum_{i=1}^n \phi_r(\mathbf{x}_i) T_r(\mathbf{x}_i) \right]^2}{\sum_{i=1}^n (\phi_r(\mathbf{x}_i))^2}; \quad r = 1, 2 \quad (14)$$

which leads to solve the following eigenvalue problems:

$$\mathbf{c}_r \phi_r = \alpha_r \phi_r; \quad r = 1, 2 \quad (15)$$

Here, the vectors ϕ_r have i -component $\phi_r(\mathbf{x}_i)$, and \mathbf{c}_r is the two-point correlation matrix:

$$c_{r,ij} = T_r(\mathbf{x}_i) T_r(\mathbf{x}_j); \quad r = 1, 2 \quad (16)$$

which is symmetric and positive definite. Being P the number of snapshots ($P = \mathcal{N}$ if we consider all the analyzed microstructures), we define the matrix \mathbf{Q}_r :

$$\mathbf{Q}_r = \begin{pmatrix} T_r^1(x_1) & T_r^2(x_1) & \cdots & T_r^P(x_1) \\ T_r^1(x_2) & T_r^2(x_2) & \cdots & T_r^P(x_2) \\ \vdots & \vdots & \ddots & \vdots \\ T_r^1(x_n) & T_r^2(x_n) & \cdots & T_r^P(x_n) \end{pmatrix}; \quad r = 1, 2 \quad (17)$$

and we have:

$$\mathbf{c}_r = \mathbf{Q}_r \cdot \mathbf{Q}_r^T; \quad r = 1, 2 \quad (18)$$

3.2. Building the POD reduced-order model

In order to obtain a reduced-order model, we first solve the eigenvalue problems (15) and select the l_r eigenvectors ϕ_i^r associated with the eigenvalues belonging to the interval defined by the highest eigenvalue α_1^r and α_1^r downscaled by a large enough number (e.g. 10^8) for both thermal problems. In practice, l_r is found to be much lower than n . These l_r eigenfunctions ϕ_i^r are then

used to approximate the solution $T_r(\mathbf{x})$. To this end, let us define the matrix $\mathbf{B}_r = [\phi_1^r, \dots, \phi_{l_r}^r]$:

$$\mathbf{B}_r = \begin{pmatrix} \phi_1^r(x_1) & \phi_2^r(x_1) & \cdots & \phi_{l_r}^r(x_1) \\ \phi_1^r(x_2) & \phi_2^r(x_2) & \cdots & \phi_{l_r}^r(x_2) \\ \vdots & \vdots & \ddots & \vdots \\ \phi_1^r(x_n) & \phi_2^r(x_n) & \cdots & \phi_{l_r}^r(x_n) \end{pmatrix}; \quad r = 1, 2 \quad (19)$$

Now, we want to compute the temperature fields for any new microstructure \mathcal{M} different of the \mathcal{N} microstructures that served for defining the reduced models. One must thus solve a linear algebraic system of the form:

$$\mathbf{H} \cdot \mathbf{T}_r = \mathbf{F}_r; \quad r = 1, 2 \quad (20)$$

A reduced-order model is then obtained by approximating \mathbf{T}_r in the subspace defined by the l_r eigenvectors ϕ_i^r :

$$\mathbf{T}_r \approx \sum_{i=1}^{l_r} \phi_i^r \zeta_i^r = \mathbf{B}_r \cdot \boldsymbol{\zeta}_r; \quad r = 1, 2 \quad (21)$$

Equation (20) then reads:

$$\mathbf{H} \cdot \mathbf{B}_r \cdot \boldsymbol{\zeta}_r = \mathbf{F}_r; \quad r = 1, 2 \quad (22)$$

or equivalently:

$$\mathbf{B}_r^T \cdot \mathbf{H} \cdot \mathbf{B}_r \cdot \boldsymbol{\zeta}_r = \mathbf{B}_r^T \cdot \mathbf{F}_r; \quad r = 1, 2 \quad (23)$$

where \mathbf{B}_r^T is the transpose of \mathbf{B}_r .

The coefficients $\boldsymbol{\zeta}_r$ defining the solution of the reduced-order model are thus obtained by solving an algebraic system of size l_r instead of n . When $l_r \ll n$, as is the case in numerous applications, the solution of (23) is thus preferred because of its much reduced size.

4. Combining thermal homogenization with reduced order modeling

In our image-based simulation, we generate a set of 100 squared microstructures $\mathcal{N} = 100$, with 100 circular inclusions of the same radius representing the fibers placed randomly in the domain. We only change the position of the fibers, allowing contacts between them and prohibiting their overlapping. Fiber volume fraction is 0.49. Each pixel of each microstructure has a known local conductivity tensor depending on whether it belongs to the fiber or to the polymer matrix.

Once we have well-defined the set of 100 microstructures, we solve both thermal problems (since we are in the case 2D) with their respective boundary conditions, obtaining two temperature fields (Eqs. (10) and (12)). After that, we apply the SVD (Singular Value Decomposition) to each to identify which are the most significant modes and so to reduce our model building a reduced basis. We will construct several reduced matrices with different numbers of significant modes l_r , to quantify which is the loss of accuracy between the reduced and the reference solution.

At this point we generate a new microstructure, \mathcal{M}_{101} , and we follow the previous homogenization procedure to compute the reference homogenized conductivity tensor.

Now we compute the reduced homogenized thermal conductivity tensor, i.e., instead of computing the temperature fields of the new microstructure, we build a reduced basis that comes from the set of 100 microstructures and from it we compute the reduced homogenized thermal conductivity tensor. We do this taking different number of significant modes coming from the SVD and we compute the relative error between both tensors to quantify the accuracy of our method.

5. Results

In this test we generate as a new microstructure one with the same characteristics as the set of 100 microstructures, i.e., we only change the position of the inclusions (Fig. 1).

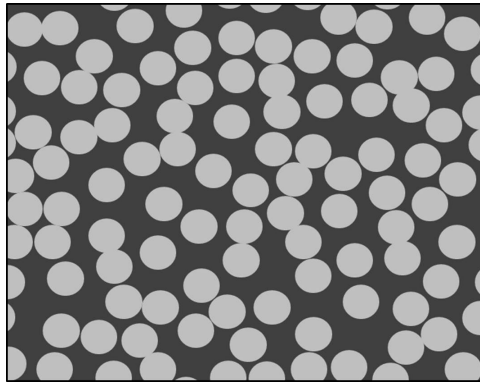


Figure 1. New microstructure obtained by changing the inclusions' position

5.1. Low contrast

We consider a local conductivity inside the fibers $k_1 = 20$ (W/mK) and a local conductivity of the matrix material $k_2 = 10$ (W/mK).

The reduced homogenized thermal conductivity tensor is computed six times, each of them taking a different number of significant modes coming from the SVD (100, 95, 75, 50, 20 and 2 modes). The relative error, depending on the number of significant modes, is estimated as:

$$\mathcal{E} = \sqrt{\frac{(\lambda_{max} - \lambda_{max}^{red})^2}{(\lambda_{max})^2}} \quad (24)$$

λ_{max} and λ_{max}^{red} being the maximum eigenvalues of the reference and the reduced homogenized thermal conductivity tensors.

One can see from Fig. 2 that the relative error corresponding to the reduced solution computed only with the first 2 modes coming from the SVD is really low.

We obtain really low relative errors when the contrast between the local conductivity of the fibers and the polymer matrix is small. So we can say that the method can be considered as a predictive method, because it allows us to predict which will be the homogenized thermal conductivity tensor of a new microstructure from a set of microstructures previously computed off-line.

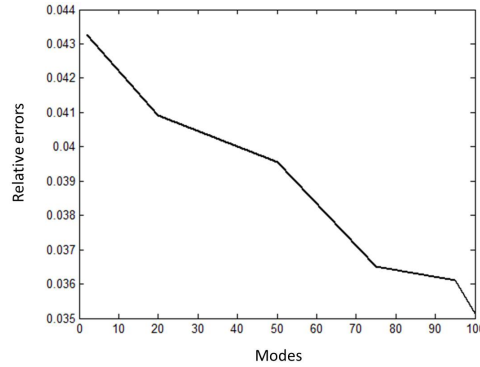


Figure 2. Relative error depending on the number of modes. Low contrast between conductivities

5.2. High contrast

For the case of high contrast between the two materials involved in the microstructure, we consider a local conductivity inside the fibers $k_1 = 20$ (W/mK) and a local conductivity of the matrix material $k_2 = 1$ (W/mK).

When the contrast between the local conductivities of both materials (fiber and polymer) is higher, the relative errors increase a lot. The reason is that we have a too large temperature gradient of the thermal modes in the region occupied by the largest conductivity material (fibers), where the temperature gradient of the solution should be the smallest one. This conflict creates significant errors when using the reduced models for calculating the homogenized conductivity.

Thus, it is necessary to correct the reduced temperature fields obtained in the prediction stage (using the reduced model) before computing their gradient for evaluating the localization tensor (correction step). For that, starting from the reduced temperatures of both fields, we apply an iterative method to correct the solution.

We have considered as a corrector three iterative methods: Jacobi, Gauss- Seidel and Conjugate Gradient.

We compare the computing time per iteration in seconds, the number of iterations required to reach a 10% error between the reference and reduced tensors, and finally the total time required to reach an error of 10% between the reference and reduced tensors in minutes.

The conjugate gradient method is the cheapest computational method.

Results in Fig. 3 show that the relative error corresponding to the reduced solution computed only with the first 2 modes coming from the SVD is really high and after applying the conjugate gradient method as a corrector method we obtain a relative error of 10% with 8 iterations.

6. Conclusions

In this work we have performed computational homogenization, introducing the reduced bases of the thermal fields coming from the reduced order modeling in the homogenization process.

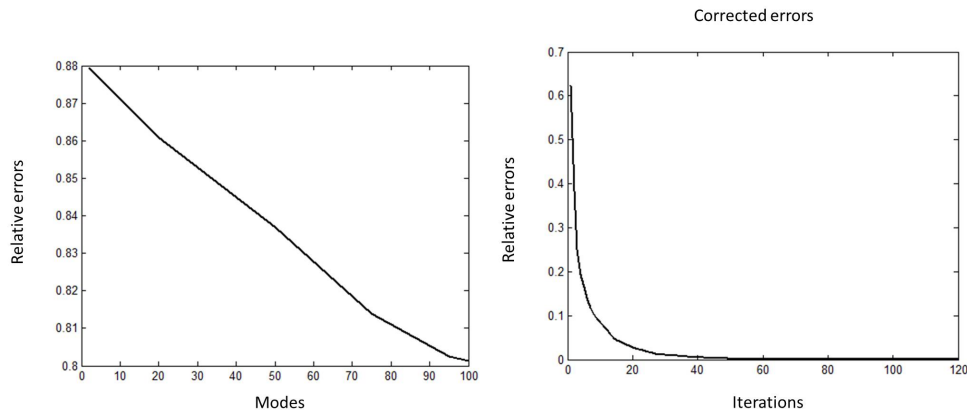


Figure 3. Relative error depending on the number of modes and Corrected relative error depending on the number of iterations. High contrast between conductivities

The homogenized thermal conductivity tensor in a complete or in a reduced way exhibits a low relative error between both tensors. We can improve the reduced computational homogenization applying correction methods, because these methods allow us to reduce the relative error due to an eventual high contrast between phases.

The next step is the application of this methodology to compute mechanical and flow properties, in particular, homogenized elasticity and permeability from digital microstructures.

References

- [1] D. Ryckelynck, F. Chinesta, E. Cueto, A. Ammar. On the a priori model reduction: Overview and recent developments. *Archives of Computational Methods in Engineering, State of the Art Reviews*, 13/1, 91-128, 2006.
- [2] F. Chinesta, A. Ammar, F. Lemarchand, P. Beauchene, F. Boust, Alleviating mesh constraints: Model reduction, parallel time integration and high resolution homogenization, *Comput. Methods Appl. Mech. Engrg.*, 197, 400413, 2008.
- [3] M. Jiang, I. Jasiuk, M. Ostoj-Starzewski, Apparent thermal conductivity of periodic two-dimensional composites, *Computational Materials Science*, 25/3, 2002, 329-338.
- [4] T. Kanit, S. Forest, I. Galliet, V. Mounoury, D. Jeulin, Determination of the size of the representative volume element for random composites: statistical and numerical approach, *Int. J. Solids Struct.* 40 (2003) 36473679.